

Topological quantum phase transitions of ultracold fermions in optical lattices

R. W. Cherng

Department of Physics, Harvard University, Cambridge, MA 02138

C. A. R. Sá de Melo

School of Physics, Georgia Institute of Technology, Atlanta Georgia 30332

(Dated: August 10, 2008)

We consider the possibility of topological quantum phase transitions of ultracold fermions in optical lattices, which can be studied as a function of interaction strength or atomic filling factor (density). The phase transitions are connected to the topology of the elementary excitation spectrum, and occur only for non-zero angular momentum pairing (p-wave, d-wave and f-wave), while they are absent for s-wave. We construct phase diagrams for the specific example of highly anisotropic optical lattices, where the proposed topological phase transitions are most pronounced. To characterize the existence of these topological transitions, we calculate several measurable quantities including momentum distribution, quasi-particle excitation spectrum, atomic compressibility, superfluid density, and sound velocities.

PACS numbers: 05.30.Fk, 03.75.Hh, 03.75.Ss

In the last few years there has been a tremendous interest in atoms loaded into optical lattices, where many known phases of standard condensed matter physics can be simulated under a tightly controlled environment. Examples of such realizations are the observation of the superfluid-to-insulator [1] transition in atomic Bose systems, metallic [2], molecular [3] and superfluid [4] phases of atomic Fermi systems. The production of quantum degeneracy of atoms and molecules in optical lattices has allowed the merger of standard condensed matter and atomic and molecular physics into a vibrant field of research called condensed atomic and molecular physics.

In standard fermionic condensed matter systems it has been very difficult to study systematically the effects of strong correlations as a function of particle density and the ratio of hopping to interaction strength, as the ability to control these parameters is generally very limited. However, in atomic systems, the strength of atom-atom interactions, the atom hopping, and the atomic filling factor in optical lattices are easily controllable and allow the exploration of a much wider phase space. In particular, the ability to control interactions relies on the existence of Feshbach resonances, which have been used to study fermions loaded into optical lattices both in the s-wave channel [4] for ^6Li , and the p -wave channel [5] for ^{40}K . More recently, p -wave Feshbach resonances in ^6Li were used to produce p -wave molecules [6, 7] in harmonically trapped systems, and it is likely that similar experiments may be attempted in optical lattices.

Currently, the only fully confirmed fermion superfluid with pairing higher than s-wave, is liquid ^3He , which is not found on a lattice. Very few lattice condensed matter candidates exist, such as the ruthenates [8], and organics [9], but since the control of carrier density, hopping and interactions in these systems is very limited, the exploration of the phase diagram of alleged p -wave lat-

tice superfluids has been hindered. Thus, the search of higher-angular momentum superfluidity in atomic systems is very important not only to help elucidate the symmetry of the order parameter in analogous condensed matter systems, but also to explore new phases that are not accessible in standard condensed matter due to the lack of control of interactions, density and hopping.

Since Feshbach resonances in optical lattices have already been observed in the p -wave channel [5], the interaction strength can be tuned continuously from weak (BCS) to strong (BEC) attraction limits. Here, we take advantage of the tunability in optical lattices to study theoretically the occurrence of unusual topological quantum phase transitions in three-dimensional but anisotropic optical lattices with superfluid order parameters in non-s-wave channels. We construct the phase diagram for anisotropic three-dimensional optical lattices in the fermion density versus interaction strength plane and identify up to five different quantum phases for non-zero angular momentum states depending on the momentum space topology of the quasiparticle excitation spectrum. For some p -wave states, we find that the quasiparticle excitations are gapless in the BCS regime, and are fully gapped in the BEC regime. To characterize the change in topology of the quasiparticle excitations, we show that the momentum distribution, atomic compressibility, superfluid density and sound velocity are non-analytic functions of the interaction strength exactly where the topological changes occur.

Hamiltonian: To describe the physics described above, we study ultracold fermions in anisotropic three-dimensional optical lattices described by the single band dispersion

$$\epsilon_{\mathbf{k}} = -2t_x \cos(k_x a) - 2t_y \cos(k_y a) - 2t_z \cos(k_z a), \quad (1)$$

Here, the hoppings $t_x > t_y > t_z$ are chosen to be different and a is the optical lattice spacing. We work with

the Hamiltonian $H = H_{kin} + H_{int}$, where the kinetic energy part is $H_{kin} = \sum_{\mathbf{k}, \alpha} \xi_{\mathbf{k}} \psi_{\mathbf{k}, \alpha}^\dagger \psi_{\mathbf{k}, \alpha}$, with $\xi_{\mathbf{k}} = \epsilon_{\mathbf{k}} - \mu$, where the chemical potential μ may contain the standard Hartree shift. The interaction part of the Hamiltonian is

$$H_{int} = \frac{1}{2} \sum_{\mathbf{k}, \mathbf{q}} \sum_{\alpha\beta\gamma\delta} V_{\alpha\beta\gamma\delta}(\mathbf{k}, \mathbf{k}') b_{\alpha\beta}^\dagger(\mathbf{k}, \mathbf{q}) b_{\gamma\delta}(\mathbf{k}', \mathbf{q}) \quad (2)$$

with $b_{\alpha\beta}^\dagger(\mathbf{k}, \mathbf{q}) = \psi_{-\mathbf{k}+\mathbf{q}/2, \alpha}^\dagger \psi_{\mathbf{k}+\mathbf{q}/2, \beta}^\dagger$, where the labels α, β, γ and δ are the pseudo-spin indices and the labels \mathbf{k}, \mathbf{k}' and \mathbf{q} represent linear momenta. We use units where $\hbar = k_B = 1$, and allow the pseudo-spins indices to take two values (pseudo-spin $S = 1/2$) corresponding to two hyperfine states labeled as $|\uparrow\rangle$ and $|\downarrow\rangle$.

In the case, where the hyperfine states (pseudo-spin indices) and the center of mass coordinates are uncoupled the model interaction tensor can be chosen to be

$$V_{\alpha\beta\gamma\delta}(\mathbf{k}, \mathbf{k}') = -V_\Gamma \phi_\Gamma(\mathbf{k}) \phi_\Gamma^*(\mathbf{k}') \Gamma_{\alpha\beta\gamma\delta}, \quad (3)$$

where the tensor $\Gamma_{\alpha\beta\gamma\delta} = \delta_{\alpha\beta} \delta_{\gamma\delta}^\dagger / 2$, for the pseudo-singlet pairing case ($S_{1,2} = S_1 + S_2 = 0$); and where $\Gamma_{\alpha\beta\gamma\delta} = \mathbf{v}_{\alpha\beta} \cdot \mathbf{v}_{\gamma\delta}^\dagger / 2$ with $\mathbf{v}_{\alpha\beta} = (i\sigma\sigma_y)_{\alpha\beta}$, for the pseudo-triplet pairing case ($S_{1,2} = S_1 + S_2 = 1$). Here, V_Γ has dimensions of energy and represents a given symmetry of the order parameter with basis function $\phi_\Gamma(\mathbf{k})$ and $\phi_\Gamma^*(\mathbf{k}')$ representative of the orthorhombic group (D_{2h}).

Self-Consistent Equations: At the saddle point, the pairing field $\mathcal{D}_\lambda(\mathbf{k}_1 + \mathbf{k}_2, \tau)$ is taken to be τ independent, and to have center of mass momentum $\mathbf{k}_1 + \mathbf{k}_2 = 0$, becoming $\mathcal{D}_0(\mathbf{k}_1 + \mathbf{k}_2, \tau) = \Delta_\Gamma \delta_{\mathbf{k}_1 + \mathbf{k}_2, 0} + \delta \mathcal{D}_0(\mathbf{k}_1 + \mathbf{k}_2, \tau)$ for the singlet case, and $\mathcal{D}_i(\mathbf{k}_1 + \mathbf{k}_2, \tau) = \eta_i \Delta_\Gamma \delta_{\mathbf{k}_1 + \mathbf{k}_2, 0} + \delta \mathcal{D}_i(\mathbf{k}_1 + \mathbf{k}_2, \tau)$ for the triplet case. The corresponding order parameter equation is

$$1 = \sum_{\mathbf{k}} |V_\Gamma| |\phi_\Gamma(\mathbf{k})|^2 \tanh(\beta E_{\mathbf{k}}/2) / 2E_{\mathbf{k}}, \quad (4)$$

The number equation is obtained from $N = -\partial\Omega/\partial\mu$, where $\beta\Omega = -\ln Z$ is the thermodynamic potential and $Z = \text{Tr}(\exp -\beta H)$ is the partition function, leading to

$$N = N_0 + N_{\text{fluct}}, \quad (5)$$

where $N_0 = \sum_{\mathbf{k}} n_{\mathbf{k}}$, and $n_{\mathbf{k}} = [1 - \xi_{\mathbf{k}} \tanh(\beta E_{\mathbf{k}}/2) / E_{\mathbf{k}}]$ is the momentum distribution. The additional term $N_{\text{fluct}} = -\partial\Omega_{\text{fluct}}/\partial\mu$, where Ω_{fluct} are Gaussian fluctuations to saddle point Ω_0 . These two equations must be solved self-consistently in order to provide the order parameter amplitude Δ_Γ , the chemical potential μ , and the quasiparticle excitation energy

$$E_{\mathbf{k}} = \sqrt{\xi_{\mathbf{k}}^2 + |\Delta_\Gamma|^2 |\phi_\Gamma(\mathbf{k})|^2}.$$

Order Parameter Symmetries: For singlet pairing the saddle point field is $\mathcal{D}_0^{(0)} = \Delta_\Gamma$, while for the triplet case it is $\mathcal{D}_i^{(0)} = \eta_i \Delta_\Gamma$, which is related to the \mathbf{d} -vector order

parameter by $d_i(\mathbf{k}) = \sum_{\mathbf{k}} \mathcal{D}_i^{(0)} \phi_\Gamma(\mathbf{k})$. For orthorhombic lattices without breaking time-reversal or parity and no coupling between pseudospins and center of mass coordinates, the only order parameters for superfluidity allowed by symmetry are: (a) $\Delta(\mathbf{k}) = \Delta_\Gamma \phi_\Gamma(\mathbf{k})$ for singlet states and (b) $\mathbf{d}(\mathbf{k}) = \hat{\eta} \Delta_\Gamma \phi_\Gamma(\mathbf{k})$ for triplet states. This implies that there are only 8 symmetries allowed for the order parameter which are consistent with the orthorhombic D_{2h} group. There are four options for the singlet case: (a) s -wave with $\Delta(\mathbf{k}) = \Delta_s$; (b) d_{xy} -wave with $\Delta(\mathbf{k}) = \Delta_{d_{xy}} XY$; (c) d_{xz} -wave with $\Delta(\mathbf{k}) = \Delta_{d_{xz}} XZ$; and (d) d_{yz} -wave with $\Delta(\mathbf{k}) = \Delta_{d_{yz}} YZ$. There are also four options for the triplet case: the \mathbf{d} -vector in momentum space for unitary triplet states in the weak spin-orbit coupling limit is characterized by one of the four states: (a) p_x -wave with $\mathbf{d}(\mathbf{k}) = \hat{\eta} \Delta_{p_x} X$; (b) p_y -wave with $\mathbf{d}(\mathbf{k}) = \hat{\eta} \Delta_{p_y} Y$; (c) p_z -wave with $\mathbf{d}(\mathbf{k}) = \hat{\eta} \Delta_{p_z} Z$; and (d) f_{xyz} -wave with $\mathbf{d}(\mathbf{k}) = \hat{\eta} \Delta_{f_{xyz}} XYZ$. Since, the Fermi surface can touch the Brillouin zone boundaries the functions X, Y , and Z need to be periodic and can be chosen to be $X = \sin(k_x a)$, $Y = \sin(k_y a)$, and $Z = \sin(k_z a)$. The unit vector $\hat{\eta}$ defines the direction of $\mathbf{d}(\mathbf{k})$. From here on we scale all energies by t_x , and choose $t_y/t_x = 0.2$ and $t_z/t_x = 0.008$ such that $t_x \gg t_y \gg t_z$ where the largest number of non-trivial phases occur.

Topological Transitions: We discuss three distinct phases based on the normal state and quasiparticle Fermi surface (FS) topologies and the nodal structure of the order parameter as a function of μ . We consider the “normal state” FS defined in the first Brillouin zone by $\xi_{\mathbf{k}} = 0$, keeping in mind the periodicity in k -space, and define the special values $\mu_1^* \equiv -2t_x - 2t_y - 2t_z$; $\mu_2^* \equiv -2t_x - 2t_y + 2t_z$; $\mu_3^* \equiv -2t_x + 2t_y - 2t_z$; $\mu_4^* \equiv -2t_x + 2t_y + 2t_z$ for filling factors $0 \leq \tilde{N} \leq 1$. The order parameter always has no nodes for the s symmetry, while the nodes for the p_i symmetry can only occur on the planes $k_i = 0, \pm\pi$ where i is x, y , or z . For the superconducting state, the intersection of the FS and order parameter nodes constitute the loci of gapless excitations, where $E(\mathbf{k}) = 0$. Since $E(\mathbf{k})$ is always gapped for the s -wave symmetry, there are no quantum phase transitions present. However, topological quantum phase transitions occur for p_i symmetries.

For all triplet p_i -wave symmetries, $E(\mathbf{k})$ is fully gapped only for $\mu < \mu_1^*$ since there is no Fermi surface. For $\mu_1^* < \mu < \mu_4^*$, the order parameter nodes intersect the Fermi surface and hence quasiparticle excitations are gapless. For $\mu_4^* < \mu$ the Fermi surface splits into two sheets that separate along k_x so that the p_x nodes no longer intersect the Fermi surface opening a gap in the excitation spectrum. However, the p_y , and p_z nodes still intersect the Fermi surface so excitations remain gapless.

Representative phase diagrams for the p_y symmetry are shown in Fig.1. There are three distinct superfluid phases characterized by Fermi surface connectivity and quasiparticle excitation spectrum: (1) no Fermi surface

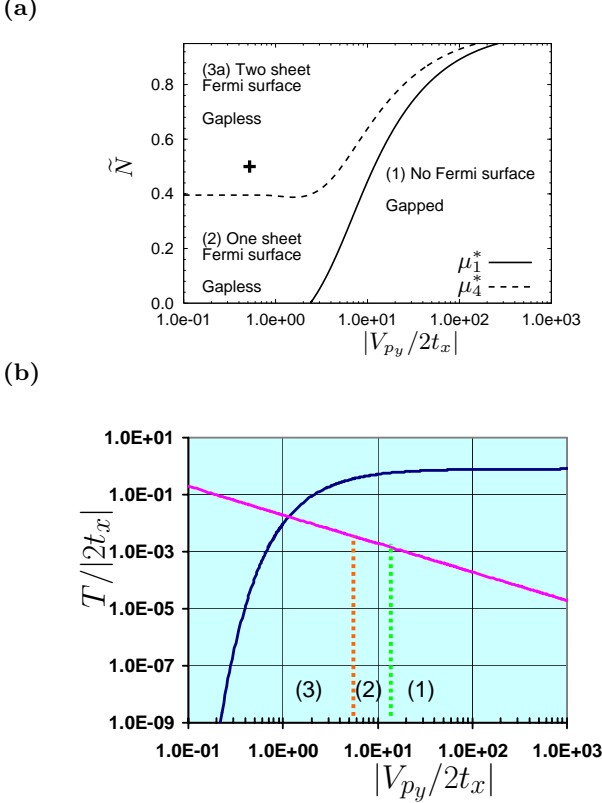


FIG. 1: a) The $T = 0$ phase diagram of filling factor \tilde{N} versus interaction V_{py} . The cross indicates the location of a suspected p -wave superfluid in highly anisotropic lattices of standard condensed matter, see Ref. [9]. b) the temperature versus interaction phase diagram at $\tilde{N} = 0.5$ (quarter filling) for the p_y symmetry. The solid lines indicate asymptotic forms of the critical temperatures for weak and strong coupling, and the dotted lines indicate the phase boundaries between topological phases of the type (1), (2) and (3). The hopping ratios used are $t_y/t_x = 0.2$, and $t_z/t_y = 0.008$.

and fully gapped for all p_i symmetries ($\mu < \mu_1^*$), (2) one sheet Fermi surface and gapless for all p_i symmetries ($\mu_1^* < \mu < \mu_4^*$), (3a) two sheet Fermi surface and gapless for p_y, p_z ($\mu_4^* < \mu$) (3b) two sheet Fermi surface and fully gapped for p_x ($\mu_4^* < \mu$). In addition, phase (2) splits into three regions using the finer classification of Fermi surface topological genus: (2i) genus zero ($\mu_1^* < \mu < \mu_2^*$), (2ii) genus one ($\mu_2^* < \mu < \mu_3^*$), (2iii) genus two ($\mu_3^* < \mu < \mu_4^*$). There are several qualitative features of interest in the phase diagrams. For a fixed low density and all triplet symmetries, the chemical potential does not go below the bottom of the band until a critical coupling is reached indicating the formation of a bound state requires a finite interaction strength, which occurs at $|V_{p_x}/2t_x| = 3.5052$, $|V_{p_y}/2t_x| = 2.3952$, and $|V_{p_z}/2t_x| = 1.8150$, for the p_x , p_y , and p_z symmetries respectively.

Momentum Distribution: While changes for s -wave are smooth, dramatic rearrangements of the momentum dis-

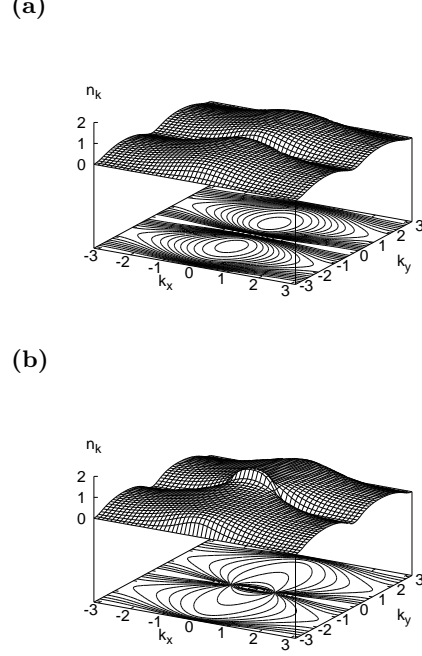


FIG. 2: Momentum distribution in the plane $k_z = 0$ for the p_y symmetry for $\tilde{N} = 0.5$ and in the vicinity of $|V_{py}/2t_x| \approx 11$ when (a) $\mu < \mu_1^*$ and (b) $\mu > \mu_1^*$. Note the jump in the momentum distribution at the origin from a) to b), signaling a topological transition at $\mu = \mu_1^*$.

tribution $n(\mathbf{k})$ accompany the topological transitions for p -wave d -wave and f -wave. For brevity, we analyze only the p_i symmetries where $i = x, y, z$. Near the points where the Fermi surface changes topology (connectivity or genus) $n(\mathbf{k}) \approx 1 + \text{sgn}(\delta\mu) - \text{sgn}(\delta\mu)\Delta_{p_j}^2 |\delta\mathbf{k}_j|^2 / (2|\delta\mu|^2)$ where $\delta\mu = \mu - \mu_j^*$ and $\delta\mathbf{k} = \mathbf{k} - \mathbf{k}_j^*$ where $j = 1, 2, 3, 4$. The momentum \mathbf{k}_j^* is the point (up to lattice periodicity) where the Fermi surface changes topology: $\mathbf{k}_1^* = (0, 0, 0)$, $\mathbf{k}_2^* = (0, 0, \pi)$, $\mathbf{k}_3^* = (0, \pi, 0)$, $\mathbf{k}_4^* = (0, \pi, \pi)$. This expansion clearly breaks down for $\delta\mu = 0$, where we find $n(\mathbf{k}) \approx 1 - |t_j| |\delta\mathbf{k}_i| / \Delta_0$ for $|\delta\mathbf{k}_j| \neq 0$, and $n(\mathbf{k}) \approx 0$ for $|\delta\mathbf{k}_j| = 0$. When μ crosses the boundaries μ_j^* , there are clear discontinuities in $n(\mathbf{k})$. Plots of $n(\mathbf{k})$ for the p_y symmetry are shown in Fig. 2 for $\tilde{N} = 0.5$ and in the vicinity of $\mu \approx \mu_1^*$ ($|V_{py}/2t_x| \approx 11$).

Compressibility and Superfluid density: The atomic compressibility and superfluid density provide additional signatures of topological quantum phase transitions in optical lattices. These quantities can be directly extracted from an analysis of quantum ($T = 0$) phase fluctuations. The effective action $S_{\text{eff}} = S_{\text{eff}}^{(0)} + \delta S_{\text{eff}}$ has a saddle point $S_{\text{eff}}^{(0)} = \beta\Omega_0$ and fluctuation $\delta S_{\text{eff}} = \beta\Omega_{\text{fluct}}$ contributions. Integrating the amplitude fluctuations in

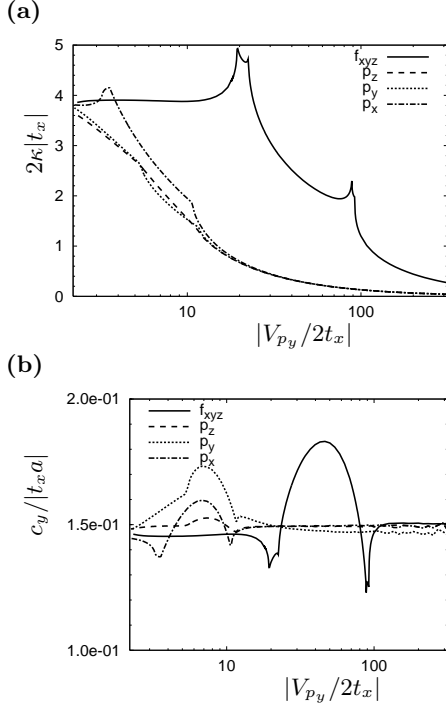


FIG. 3: Plots of (a) atomic compressibility κ and (b) sound velocity c_y versus interaction V_{p_y} for the p_y -symmetry at zero temperature. The parameters are the same as in Fig. 1

δS_{eff} leads to the phase only action

$$\delta S_{\text{phase}} = \frac{1}{8} \sum_{q, \omega_n} [A(\omega_n)^2 + \rho_{ij} q_i q_j] \theta(q) \theta(-q), \quad (6)$$

with $\theta(q)$ being the phase field of the order parameter and $A = N^2 \kappa / V$, where $\kappa = -\frac{1}{V} \left(\frac{\partial V}{\partial P} \right)_{T, N} = \frac{1}{N^2} \left(\frac{\partial N}{\partial \mu} \right)_{T, V}$ is the atomic compressibility and $\rho_{ij} = V^{-1} \sum_{\mathbf{k}} [n_{\mathbf{k}} \partial_i \partial_j \xi_{\mathbf{k}}]$ is the superfluid density tensor. Notice that ΔS does not only give κ and ρ_{ij} but also the phase-only collective mode (sound) velocity $\omega(\mathbf{k}) = \sqrt{c_x^2 q_x^2 + c_y^2 q_y^2 + c_z^2 q_z^2}$, where $c_x^2 = \rho_{xx}/A$, $c_y^2 = \rho_{yy}/A$ and $c_z^2 = \rho_{zz}/A$, when the analytic continuation $i\omega_n \rightarrow \omega + i\delta$ is performed.

Measurement of two quantities out of three (sound velocity, superfluid density and compressibility) can yield the third one. In particular, the techniques used to measure accurately the sound velocity of superfluid fermions in harmonic traps [10, 11] and to measure compressibility [12] can be used in the lattice case. In Fig. 3, we show (a) the atomic compressibility κ , and (b) the sound velocity $c_y = \sqrt{(\rho_{yy}V)/(N^2\kappa)}$ along the y -direction. Notice the clear non-analytic behavior in these two quantities when the phase boundaries between different topological phases are crossed.

The non-analytic behavior of the momentum distribution, sound velocity and compressibility, as function of interaction strength or density (not shown) character-

izes the topological quantum phase transition described. Since topological transitions occur without a change in symmetry, they can not be classified under Landau's scheme, however discontinuities occur in the third derivative of the thermodynamic potential (first derivative of compressibility), and the transition can be identified as a third-order transition under Ehrenfest's classification. This type of topological quantum phase transition belongs to a class of transitions first envisioned by Lifshitz [13] for non-interacting Fermi systems, where the Fermi surface changes its topology of under the influence of external pressure. Lifshitz's original idea was extended to continuum theories of interacting fermions by Volovik [14] in the context of ^3He , where topological invariants were constructed for topological changes in the quasiparticle excitation spectrum, but thermodynamic signatures were not analyzed. Here, we generalized their pioneering work to the case interacting fermions in a lattice, and described thermodynamic and transport signatures of topological quantum phase transitions in the superfluid phase.

Summary: We studied topological quantum phase transitions of ultracold fermions in optical lattices. For brevity, we focused on quasi-one-dimensional optical lattices, where the nature of the topological transitions in the superfluid state is most dramatic. We classified the quantum superfluid phases in accordance to their Fermi surface topologies and quasiparticle excitation spectrum. We showed that for s -wave superfluids there is no phase transition, but for p -wave (d -wave or f -wave) superfluids, quantum phase transitions of topological nature can occur, in particular from a phase with gapless quasiparticle excitations (BCS regime) to a phase of with gapful quasiparticle excitations (BEC regime). Finally, we showed that non-analytic behavior of the momentum distribution, compressibility, sound velocities and superfluid density tensor as a function of interaction strength characterize well the topological phase transitions for p_x , p_y and p_z , and f_{xyz} pairing symmetries. We would like to thank NSF for support (Grant No. DMR-0709584)

-
- [1] I. Bloch, Nat. Phys. **1**, 23 (2005). Dynamics, and Interactions
 - [2] M. Köhl *et al.*, Phys. Rev. Lett. **94**, 080403 (2005).
 - [3] T. Stöferle *et al.*, Phys. Rev. Lett. **96**, 030401 (2006).
 - [4] J. K. Chin *et al.*, Nature **443**, 961 (2006).
 - [5] K. Günter *et al.*, Phys. Rev. Lett. **95**, 230401 (2005).
 - [6] J. Fuchs, *et al.* e-print arXiv:0802.3262 (2008).
 - [7] Y. Inada, *et al.* e-print arXiv:0803.1405 (2008).
 - [8] A. P. Mackenzie and Y. Maeno Rev. Mod. Phys. **75**, 657 (2003)
 - [9] Wei Zhang, and C. A. R. Sá de Melo, Adv. Phys. **56**, 546 (2007).
 - [10] M. Bartenstein *et al.*, Phys. Rev. Lett. **92**, 203201 (2004).

- [11] J. Kinast, A. Turlapov, and J. E. Thomas, Phys. Rev. Lett. **94**, 170404 (2005).
- [12] I. Bloch, private communication.
- [13] I. M. Lifshitz, Zh. Eksp. Teor. Fiz. **38**, 1569 (1960).
- [14] G. E. Volovik, *Exotic Properties of Superfluid ^3He* (World Scientific, Singapore, 1992). See also recent review, e-print arxiv:cond-mat/0601372.